Preparation and evaluation of carbon-supported catalysts for ethanol oxidation

A. Bonesi · M. Asteazaran · M. S. Moreno · G. Zampieri · S. Bengio · W. Triaca · A. M. Castro Luna

Abstract Supported PtSnIr/C, PtSn/C, and IrSn/C catalysts with potential application in a direct alcohol fuel cell were prepared by chemical reduction employing Pechini methodology. The catalyst particles were characterized by high-resolution transmission electron microscopy, energy-dispersive X-ray spectroscopy, and X-ray photoelectron spectroscopy (XPS). Linear sweep voltammetry (LV), chronoamperometry, and electrochemical impedance spectroscopy (EIS) measurements were performed by using a glassy carbon working electrode covered with the catalyst in a 1 M ethanol+0.5 M H_2SO_4 solution at 60 °C. It was demonstrated through XPS that PtSnIr/C and IrSn/C contain both IrO_2 and SnO_2. LV and chronoamperometry show a better catalytic behavior for ethanol oxidation on PtSnIr/C in the low-potential region and the improvement is attributed to the presence of both Sn and Ir oxides. The EIS accurately established that PtSnIr/C improved ethanol oxidation at lower potentials than PtSn/C.

Keywords Platinum · Iridium · Tin · Ethanol · DEFC · Nanoparticles · Electrochemical impedance spectroscopy

A. Bonesi · M. Asteazaran · W. Triaca · A. M. Castro Luna (✉)
Instituto de Investigaciones Fisicoquímicas Teóricas y Aplicadas (INIFTA), Facultad de Ciencias Exactas, UNLP-CONICET, La Plata, Buenos Aires, Argentina
e-mail: castrolu@gmail.com

A. M. Castro Luna
e-mail: castrolu@inifta.unlp.edu.ar

M. Asteazaran · A. M. Castro Luna
Centro de Investigación y Desarrollo en Ciencia y Tecnología de Materiales (CITEMA), Facultad Regional La Plata, UTN, La Plata, Argentina

M. S. Moreno · G. Zampieri · S. Bengio
Centro Atómico Bariloche, Comisión Nacional de Energía Atómica (CAB-CNEA), Bariloche, Argentina

Introduction

Fuel cells that employ liquid alcohols such as a direct ethanol fuel cell (DEFC) are attractive to power portable devices because their theoretical cell voltage is similar to that obtained when hydrogen is oxidized [1–3] and in the case of ethanol, its complete electro-oxidation involves a 12-electron process. Unlike hydrogen, ethanol is easy to handle, transport, and store and no previous reformer system is necessary. Nevertheless, DEFC undergoes slow kinetics of alcohol oxidation on electrode surfaces. Efficiency is currently quite low for that cell [4]. To achieve the maximum chemical energy from an alcohol molecule, it should be completely oxidized to CO_2. Research into alcohol fuel cell catalysis is focused primarily on increasing the catalytic efficiency of the electrode materials [5]. Platinum is considered as the most active catalyst for ethanol oxidation at low temperature. However, the main problem in achieving an efficient conversion is that ethanol oxidation can be conducted through different paths. Thus, large amounts of partially oxidized products such as acetaldehyde and acetic acid have been detected at low temperature as the main products in ethanol oxidation (EO) [5, 6]. Moreover, strongly adsorbed species such as CO and CH_x, which are difficult to convert to CO_2, block the surface and hinder further alcohol adsorption causing low-power densities at DEFC. A good ethanol catalyst should have a great capacity to electro-oxidize ethanol to CO_2 and water, but Pt alone shows a low capability to sufficiently favor the C–C rupture of the ethanol molecule. Therefore, the electrocatalytic concern is to cope with a material that facilitates ethanol complete oxidation and shifts the onset oxidation potential to lower values.

It appears that an improvement in EO electrocatalysis is possible with multifunctional Pt-based combinations. The superior performance of binary or ternary Pt-based catalysts relative to a pure Pt catalyst has been explained in terms of

two models: the bifunctional mechanism and the ligand effect. In the bifunctional mechanism model, the added components to Pt provide the oxygen-containing species required for the oxidative removal of adsorbed CO-like species. The ligand effect is considered as a modification of the Pt electronic structure by the presence of the added atoms, therefore the adsorbed residues are less strongly bonded to Pt and consequently easier to remove [5]. In case of PtM alloy formation, the alien atom M, can go into the Pt crystal net modifying the Pt–Pt distance and favoring adsorption and breaking of the ethanol molecule [7]. Thus, it is well known that the addition of Sn to Pt enhances the activity for EO particularly at lower potentials as compared to that obtained with Pt catalyst. Jiang et al. [8] established a correlation between the structures of PtSn alloy and $PtSnO_2$ prepared by the polyol method and postulated that SnO_2 in the vicinity of Pt has the ability to promote the oxidation of CO-like species resulting from alcohol oxidative adsorption. On the other hand, the addition of a fourth metal (Ir) in the ternary PtMnCu/C and PtMnMo/C leads to quaternary alloys with better catalytic activity towards EO according to Amman et al. [9]. It has also been claimed by Chen et al. that the presence of IrO_2 improves methanol oxidation [10]. Moreover, Cao et al. claimed that the combination Ir_3Sn is a promising alternative choice of anode catalyst for DEFC [11]. Furthermore, a significant improvement in ethylene glycol electro-oxidation with multilayer PtIr catalysts has been reported [12]. The addition of Ir seems to speed up the activation of the C–H bonds in methanol electrooxidation [13]. In order to get a deeper knowledge of the ethanol oxidation reaction, it is important to determine the role of the catalyst components and what are their beneficial contributions to EO catalysis.

The aim of this work has been to synthesize and characterize Pt-based materials such as binary PtSn/C, IrSn/C, and ternary PtSnIr/C alloys and to determine the catalyst with the best activity for ethanol oxidation.

Experimental

Catalysts containing Pt, Sn, and Ir with a fixed total metal loading on carbon of 40 wt% were synthesized employing ethylene glycol (EG) as a reactant and reducing agent together with citric acid (CA) in line with the Pechini methodology [14, 15]. Briefly, Pt, Ir, and Sn polymeric precursors were prepared separately by employing metallic salts, namely, H_2PtCl_6, $IrCl_3 \cdot xH_2O$, and Sn citrate, dissolved in a mixture of EG and CA at 90 °C and the mixture was kept under vigorous stirring for 2–3 h composing a polyester network that contains the metallic ions homogeneously distributed. The CA/EG/metal molar ratio is 4:16:1 for all the polymeric precursors. It appears that the citric chelate helps to prevent particle aggregation in a certain extent and induce nanoparticles to get high dispersion.

To obtain the supported catalysts, appropriate amounts of the polymeric precursors were dissolved in ethanol and a calculated amount of the functionalized carbon black support was added. Finally, the mixture precursor solution/carbon was homogenized in an ultrasonic bath and then calcinated at different temperatures under an air atmosphere, using a temperature program reaching 350 °C to get rid of organic residues [14]. Additionally, the functionalization of the support was achieved after an oxidative treatment in 70 % HNO_3 solution at 140 °C for 2 h according to [16].

The physical characterization of the materials was accomplished by high-resolution transmission electron microscopy (HRTEM), energy dispersive spectroscopy (EDS), and X-ray photoelectron spectroscopy (XPS).

For the electrochemical characterization, a conventional three-electrode cell was employed. The working electrode consisted of a glassy carbon disk (0.071 cm^2 geometric area) covered by a thin layer of catalyst (28 μg cm^{-2} Pt loading) embedded in a Nafion polymer electrolyte film (0.1 μm thick) [17]. A Pt foil of ca 1 cm^2 geometric area was used as counter electrode and a saturated calomel electrode as reference electrode. In this work, the potentials are referred to that of the reversible hydrogen electrode.

The supporting electrolyte was 0.5 M H_2SO_4 and the working solutions were 1 M C_2H_5OH+0.5 M H_2SO_4 solutions. After assembling, the composite catalytic disk electrode was cycled in 0.5 M H_2SO_4 for 5 min at 0.10 V s^{-1} between 0.05 and 1.24 V to clean the surface. Real areas were determined by considering the anodic charge corresponding to the CO-stripping peak and assuming that CO is linearly adsorbed on one Pt site and taking into account that 420 μC is equivalent to 1 cm^2.

To determine the catalytic activity of the synthesized materials, current–potential curves for EO were recorded at 0.01 V s^{-1}. Alcohol was added to the supporting electrolyte at 0.05 V and its oxidation was measured. The temporal stability of the electrode at 0.5 V was determined by chronoamperometry. The current densities are referred to the CO calculated real area. Electrochemical impedance spectroscopy (EIS) was also employed to identify the materials with the best EO performance. The impedance spectra were recorded by polarizing in a constant voltage mode from 0.4 to 0.85 V at frequencies from 100 kHz to 10 mHz. The amplitude of the applied potential perturbation was 0.010 V. All electrochemical measurements were performed at 60 °C.

Prior to each EIS measurement, the electrolyte was replaced by fresh solution and the electrode was cycled to get a clean and reproducible surface. A 30-min holding time was applied at each potential to approach a near steady state before the data were collected.

Results and discussion

Physicochemical characterization

HRTEM and SEM-EDS analysis

HRTEM images of (a) PtSn/C, (b) IrSn/C, and (c) PtSnIr/C catalysts together with the corresponding histograms are shown in Fig. 1. All catalysts have a good dispersion on the carbon support and from the histograms it is inferred that the nanoparticles are well-dispersed on carbon support. The average particle size for PtSn/C was ca 4.5 nm, for IrSn/C was around 6.5 nm, and for PtSnIr/C was 5.12 nm. It is possible that the Pechini methodology tends to produce agglomeration of particles during the calcination treatment at 350 °C. One of the causes of bad performance of a catalyst is related to activity loss due to the particle agglomeration.

The atomic percentages of the component in the binary and ternary catalysts, which are listed in Table 1, have been determined by EDS and XPS. It can be highlighted that EDS is a surface technique that goes through less than 10 μm, whereas XPS measures the elemental composition of the surface from the top to 10 nm depth. From Table 1, it can be noted that a significant surface Sn enrichment by segregation of Sn onto the surface, due to the great affinity of Sn for oxygen the migration of Sn of the catalyst towards the surface, occurs [18].

XPS analysis

The XPS analysis for the catalysts PtSnIr/C and IrSn/C are shown in different binding energy regions. Thus, for PtSnIr/C, the sets of peaks with binding energies ranging from 70 to 80 eV correspond to Pt 4f core level and those

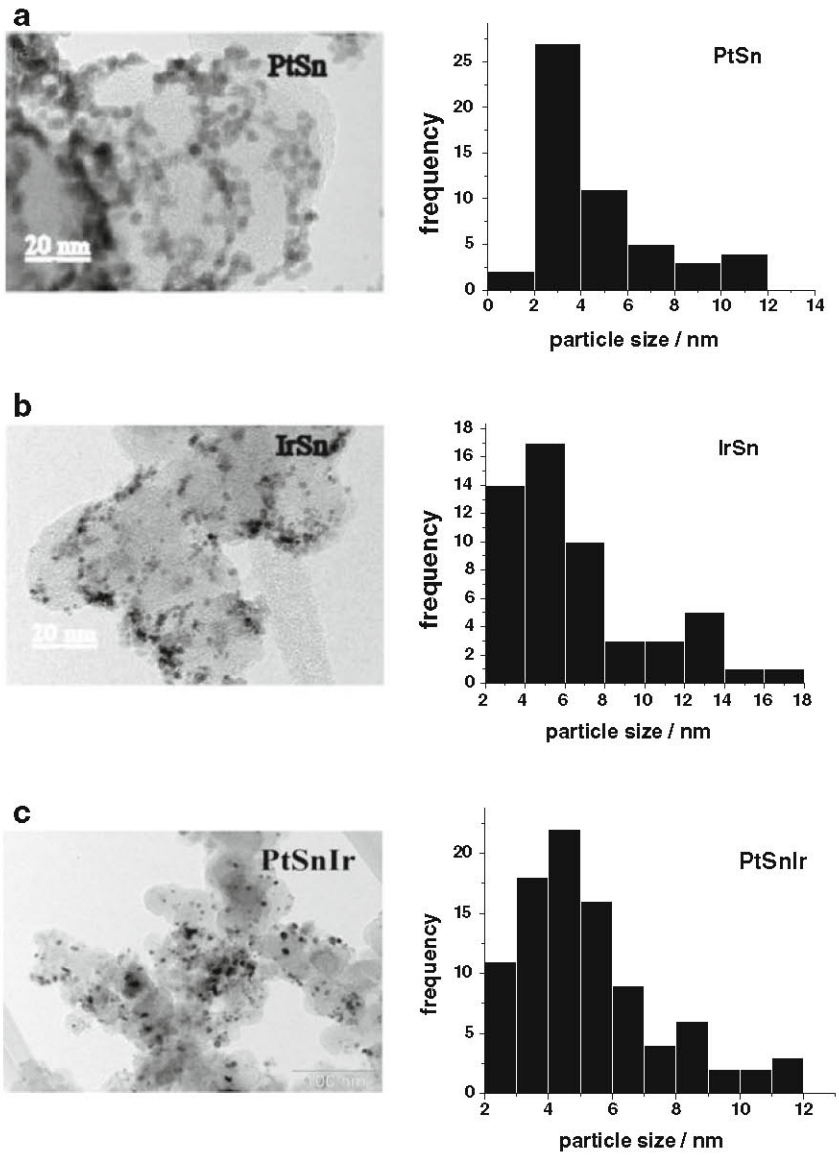

Fig. 1 TEM micrographs and histograms for **a** PtSn/C, **b** IrSn/C, and **c** PtSnIr/C catalysts

Table 1 EDX composition of the synthesized catalysts and CO stripping active area

Catalyst	XPS % at composition	EDX % at composition	real active surface area (COstripping)/ cm^2
PtSnIr	$Pt_{1.42}Sn_1Ir_0$	$Pt_3Sn_{0.48}Ir_{0.64}$	1.21
IrSn	Ir_1 $Sn_{1.68}$	–	0.7
PtSn	–	$Pt_3Sn_{1.07}$	1.18

between 60 and 68 eV are attributed to Ir 4f core level (Fig. 2a); both complex peaks can be deconvoluted into two peaks. Thus, for Ir the peak at around 61.1 eV is ascribed to Ir (0), and the peak at *ca*. 63 eV to IrO_2. The relative intensities of the components were 48 and 52 %, respectively. The deconvoluted spectra for Pt with binding energy at 71.6 and ca 74.3 eV were assigned to Pt (0) and PtO_2, respectively. The relative intensities of the Pt components were 85 and 15 %, respectively. The metallic component Pt (0) is the major component in the ternary catalyst.

In Fig. 2b, the Sn $3d_{5/2}$ XPS spectrum of PtSnIr/C sample, in the binding energy region between 480 and 490 eV, confirms that Sn is mostly in an oxidized state as SnO_2, according with the well-known oxophilicity of Sn [19].

For the catalyst IrSn/C, the Ir 4f core level binding energy region is shown in Fig. 2c. Again, the original signal for Ir 4f core level is deconvoluted into two peaks; one at 61.1 eV, attributed to Ir (0), and the other at 63.2 eV, assigned to Ir (IV). The relative intensities of the components were 70 and 30 %, respectively. The Sn $3d_{5/2}$ core level binding energy region is depicted in Fig. 2d and also confirmed that Sn is mostly in an oxidized state SnO_2. Previous reports have shown that the electronegativity of Sn was lower than that of Ir, which indicates that SnO_2 should be less acidic than

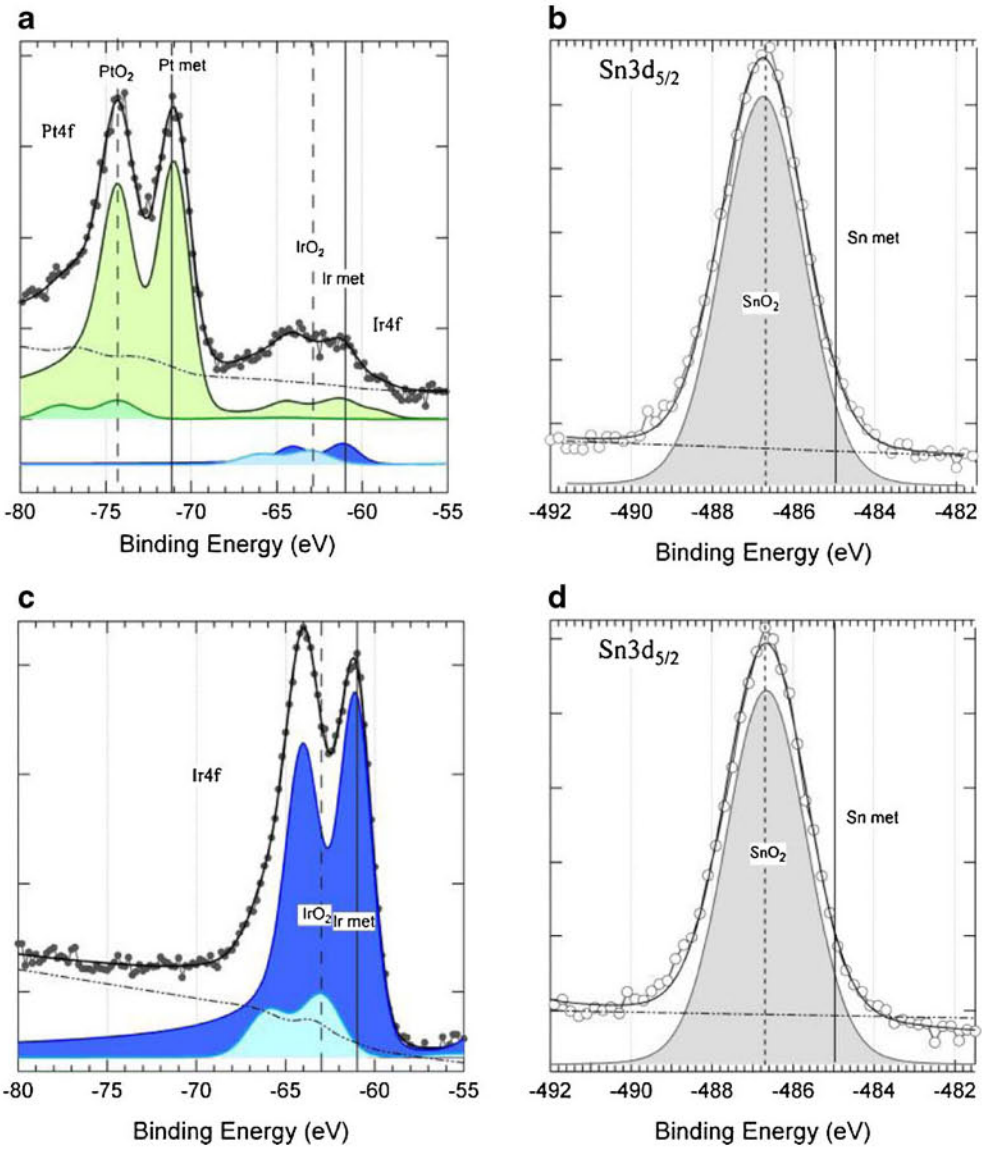

Fig. 2 XPS spectra for PtSnIr **a** in the Pt 4f and Ir4f energy region, **b** in the Sn $3d_{5/2}$ for IrSn/C, **c** in the Ir 4f energy region, and **d** in the Sn $3d_{5/2}$

IrO_2 [20]. Consequently, the addition of SnO_2 can effectively remove adsorbed hydroxyl species and increase the utilization ratio of the other active elements.

Electrochemical characterization

Linear sweep voltammetry

In Table 1, the real area values for all the studied catalysts obtained from de CO stripping experiences are shown. The areas determined for PtSnIr/C and PtSn/C are higher than corresponding to IrSn/C. It can be inferred from the composition of the catalysts that the increase on the electroactive area can be attributed to the presence of Pt. The CO stripping curves show an onset potential shift to lower values on the Pt-based catalysts. It can be highlighted that Stamenkovic et al. [21] claim that Sn atoms located near Pt sites may affect the adsorption characteristic of Pt atoms due to changes in the local potential of zero charge of Pt atoms near the Sn atoms, promoting OH adsorption at Pt sites at a lower electrode potential than pure Pt and therefore the onset of CO oxidation starts at lower potentials.

Chen et al. found that the presence of IrO_2 thin film in Ti/IrO2/Pt nanoparticles promotes CO oxidation at a much lower electrode potential than Pt [10]. The analysis of methanol oxidation on PtRuOsIr alloys revealed that the addition of Ir appears to accelerate the activation of the C–H bonds of the alcohol [20].

The linear sweep voltammograms at 0.010 V s^{-1} and 60 °C for EO, employing PtSn/C, IrSn/C, and PtSnIr/C as catalysts are shown in Fig. 3a. It can be seen that PtSnIr/C catalyst shows the highest performance for EO. The higher catalytic activity follows the order PtSnIr/C>PtSn/C> IrSn/C. At first glance, it is supposed that there is a synergic effect between Pt, Ir, and Sn to carry out the EO reaction. Besides, straightforward participation of the oxide–metal interface in the catalytic alcohol oxidation process has been recognized by different researchers [13, 22] It has been also demonstrated that metal oxides can help in the dissociation of water [23]. Thus, the higher activity for EO employing the PtSnIr/C catalyst can be attributed to a synergetic effect of Sn (or SnO_2) and Ir (or IrO_2) on the surface causing the dissociation of water and providing the extra oxygen required for the oxidative removal of species adsorbed on adjacent Pt-active sites. It is important to stress that many O-adsorbing metals can produce negative effects, e.g., inhibit alcohol adsorption or may be not sufficiently stable for long-term use in acid media [24].

Chronoamperometry

In Fig. 3b, the chronoamperograms at 0.50 V for EO show highest currents for PtSnIr/C catalyst. The current values, which are very high at the beginning, decrease rapid before reaching quasistabilization. A soft decrease is observed at longer times. The temporal stabilization of the oxidation ethanol current is an important factor for employing the catalysts in a DEFC [2].

Electrochemical impedance spectroscopy

The electrochemical impedance spectra carried out at 0.50 V for PtSnIr/C and PtSn/C (Fig. 4a) and at 0.55 V for PtSnIr/C and IrSn/C (Fig. 4b) are shown as Nyquist plots. In both plots, it can be observed that the smaller semicircle fitted the PtSnIr/C data. It is generally predicted that the lower the charge transfer resistance, the better the catalyst. Some researchers claimed that Sn and Ir activate water dissociation at lower potentials than on platinum, leading to the formation of OH species and promoting EO according to the bifunctional mechanism [25].

Impedance spectra of EO for PtSnIr/C at 60 °C and different applied potentials varying from 0.40 to 0.850 V are shown in Fig. 4c. At 0.40 V, a semicircle in the complex plane with impedance values in the fourth quadrant at low frequency is observed. It is assumed that ethanol is adsorbed and dehydrogenated on Pt sites to produce intermediate species, which are difficult to oxidize. At 0.45 V, the

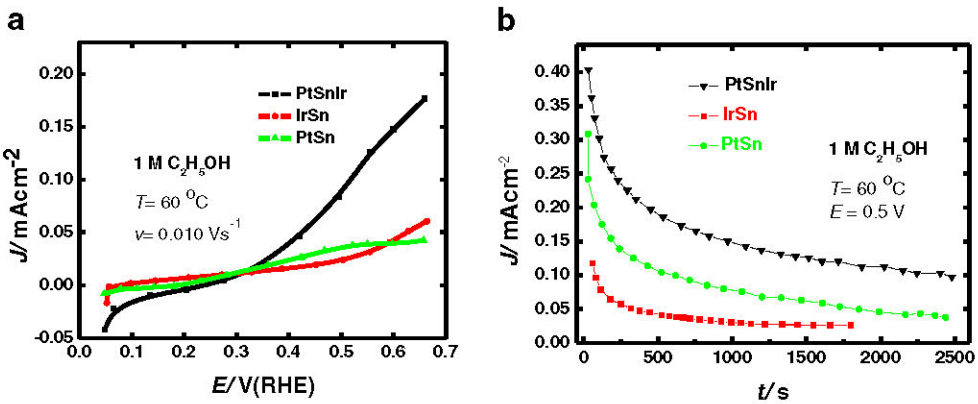

Fig. 3 **a** Linear sweep voltammetry at 0.010 V s^{-1} for EO at 60 °C for PtSnIr/C, PtSn/C and IrSn/C; **b** chronoamperograms at E= 0.50 V and 60 °C for PtSnIr/C, PtSn/C and IrSn/C

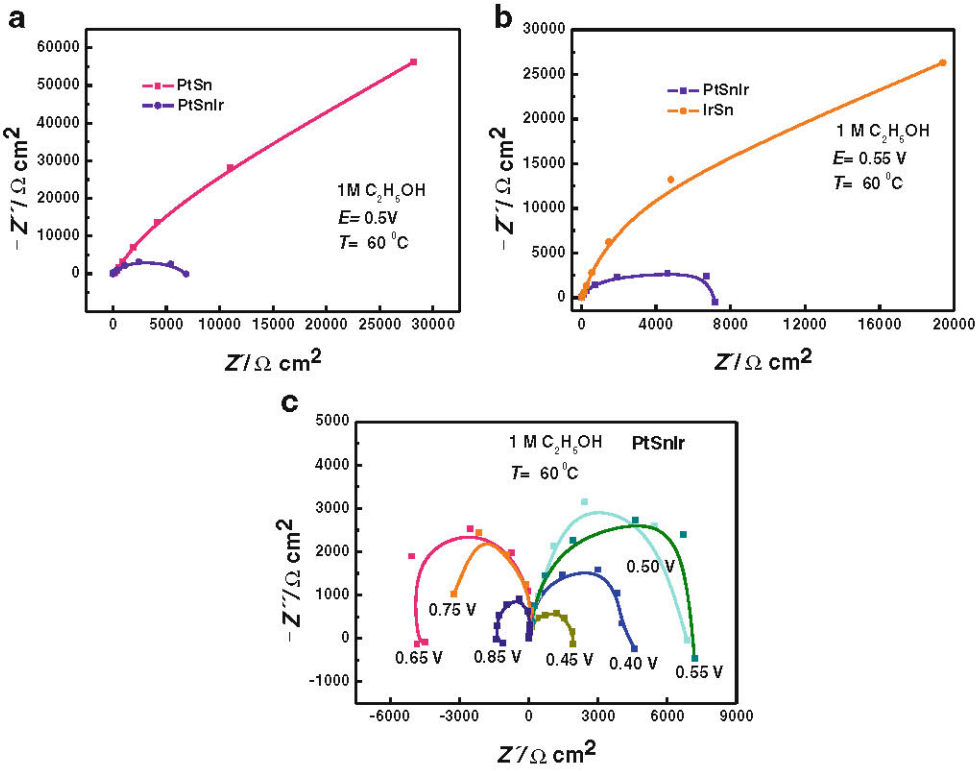

Fig. 4 EIS spectra for EO at 60 °C for **a** PtSn/C and PtSnIr/C at E=0.50 V and **b** PtSnIr/C and IrSn/C at E=0.55 V and (**c**) PtSnIr/C at E=0.40 V (*blue*), 0.45 V (*moss green*), 0.50 V (*cyan*), 0.55 V (*green*), 0.65 V (*pink*), 0.75 V (*orange*), 0.85 V (*dark blue*)

diameter of the semicircle decreases indicating that the charge transfer rate increases with increasing potential. In addition, the inductive loop at low frequencies can be attributed to changes in the rate-determining step. Thus, the oxidation of adsorbed intermediates is expected [13, 15, 23, 24]. Liang et al. claimed that the microwave-irradiated polyol plus annealing prepared PtRuIr/C catalyst displayed an enhanced activity for CO_{ads} electro-oxidation [26]. The reaction rate increases with potential and there is a competition between fresh ethanol and water molecules for the liberated Pt sites and thus as the oxidation reaction progresses, the Pt catalytic sites are occupied either by new ethanol molecules or water molecules. It is well established that to accomplish the oxidation of ethanol, the reactants and adsorbed intermediates need to assemble M–OH species produced by dissociative adsorption of H_2O on the catalyst surface. When the potential increases over 0.65 V, a sudden change in the impedance pattern happens with the arcs reversing to the second and third quadrants, and subsequent potential increments from 0.65 to 0.85 V show smaller arcs diameter [27]. A similar observation has already been reported by Melnick et al. [28] for methanol electro-oxidation on Pt, which was related to the formation of oxygen species through water activation on the Pt surface. It is concluded that at higher potentials, the strong adsorption of O-species on the catalyst surface, inhibits further EO. The role of cocatalysts as oxygen suppliers is an important factor to consider in the catalytic activity determination and it is strongly dependant on the nature of the cocatalysts as it has been shown in previous work [16].

Conclusions

- The binary IrSn/C and the ternary PtSnIr/C supported catalysts synthesized by the Pechini method contain Sn and Ir oxides, according to physicochemical analysis. The particle size and distribution of the catalysts on carbon reveal that the Pechini method is adequate to obtain binary and ternary catalysts.
- The electrochemical characterization shows that for PtSnIr/C catalyst, the onset potential for EO starts at lower potentials than for PtSn/C and IrSn/C catalysts.
- By applying different potentials in the electrochemical impedance analysis, it is possible to describe the various stages of the ethanol oxidation reaction on PtSnIr, i.e., the dehydrogenation at E<0.50 V and oxidation of carbon residues E>0.50 V and inhibition by through oxide formation for E≥0.65 V.
- The EIS study gives a clear evidence of the potential range where PtSnIr/C is a useful catalyst for EO.

Acknowledgments This work was supported by Consejo Nacional de Investigaciones Científicas y Técnicas (CONICET), Agencia Nacional de Promoción Científica y Tecnológica, Comisión de Investigaciones Científicas de la Provincia de Buenos Aires (CIC), and Universidad

Tecnológica Nacional (UTN-FRLP). AMCL is member of the research career at CIC.

References

1. Liu H, Song C, Zhang L, Zhang J, Wang H, Wilkinson DP (2006) A review of anode catalysis in the direct methanol fuel cell. J Power Sources 155:95–110
2. Gasteiger HA, Baker DR, Carter RN, Gu W, Liu Y, Wagner FT, Yu PT (2010) Electrocatalysis and catalyst degradation challenges in proton exchange membrane fuel cells hydrogen energy. In: Stolten D (ed). Wiley: Weinheim. ISBN:9783-527-32711-9
3. Aricò AS, Baglio V, Antonucci V (2009) Direct methanol fuel cells: history, status and perspectives. In: Liu H, Zhang J (eds) Electrocatalysis of direct methanol fuel cells. Wiley, Weinheim. ISBN 978-3-527-32377-7
4. Purgato FLS, Pronier S, Olivi P, De Andrade AR, Léger JM, Tremiliosi-Filho G, Kokoh KB (2012) Direct ethanol fuel cell: electrochemical performance at 90 °C on Pt and PtSn/C electrocatalysts. J Power Sources 198:95–99
5. Antolini E (2007) Catalysis for direct ethanol fuel cells. J Power Sources 170:1–12
6. Heinen M, Jusys Z, Behm RJ (2010) Ethanol, acetaldehyde and acetic acid adsorption/electrooxidation on a Pt thin film electrode under continuous electrolyte flow: an in situ ATR-FTIRS flow cell study. J Phys Chem C 114:9850–9864
7. Colmati EF, Antolini E, Gonzalez ER (2006) Effect of temperature on the mechanism of ethanol oxidation on carbon supported PtRu and Pt_3Sn electrocatalysts. J Power Sources 157:98–103
8. Jiang L, Colmenares L, Jusys Z, Sun GQ, Behm RJ (2007) Ethanol electrooxidation on novel carbon supported Pt-SnO_x-C catalysts with varied Pt:Sn ratio. Electrochim Acta 53:377–389
9. Ammam M, Easton EB (2012) Quaternary PtMnCuX/C (X=Fe, Co, Ni, and Sn) and PtMnMoX/C (X=Fe, Co, Ni, Cu and Sn) alloys catalysts: synthesis, characterization and activity towards ethanol electrooxidation. J Power Sources 215:188–198
10. Chen A, La Russa DJ, Miller B (2004) Effect of the iridium oxide thin film on the electrochemical activity of platinum nanoparticles. Langmuir 20:9695–9702
11. Cao L, Sun G, Li H, Xin Q (2007) Carbon-supported IrSn catalysts for a direct ethanol fuel cell. Electrochem Commun 9:2541–2546
12. Freitas RG, Antunes EP, Christensen PA, Pereira EC (2012) The influence of Ir and Pt_1Ir_1 structure in metallic multilayers nanoarchitectured electrodes towards ethylene glycol electro-oxidation. J Power Sources 214:351–357
13. Calegaro ML, Suffredini HB, Machado SAS, Avaca LA (2006) Preparation, characterization and utilization of a new electrocatalyst for ethanol oxidation obtained by the sol–gel method. J Power Sources 156:300–305
14. Ribeiro J, dos Anjos DM, Kokoh KB, Coutanceau C, Leger JM, Olivi P, de Andrade AR, Tremiliosi-Filho G (2007) Carbon-supported ternary PtSnIr catalysts for direct ethanol fuel cell. Electrochim Acta 52:6997–7006
15. Pechini PM, United States Patent Office 1967, 3330697
16. Bonesi AR, Moreno MS, Triaca WE, Castro Luna AM (2010) Modified catalytic materials for ethanol oxidation. Int J Hydrogen Energy 35:5999–6004
17. Paulus UA, Schmidt TJ, Gasteiger HA, Behm RJ (2001) Oxygen reduction on a high-surface area Pt/Vulcan carbon catalyst: a thin-film rotating ring-disk electrode study. J Electroanal Chem 495:134–145
18. Bates SP (2002) Full-coverage adsorption of water on SnO2 (110): the stabilization of the molecular species. Surf Sci 512:29–36
19. Tayal J, Rawat B, Basu S (2011) Bimetallic and trimetallic PtSn/C, PtIr/C, PtIrSn/C catalysts for electro-oxidation of ethanol in direct ethanol fuel cell Int. J Hydrogen Energy 36:14884–14897
20. Gurau B, Viswanathan R, Liu R, Lafrenz T, Ley K, Smotkin ES, Reddington E, Sapienza A, Chan BC, Mallouk T, Sarangapani S (1998) Structural and electrochemical characterization of binary, ternary, and quaternary platinum alloy catalysts for methanol electro-oxidation. J Phys Chem B 102:9997–10003
21. Stamenkovic V, Arenz M, Blizanac BB, Mayrhofer KJJ, Ross PN, Markovic NM (2005) In situ CO oxidation on well characterized Pt_3Sn(hkl) surfaces: a selective review. Surf Sci 576:145–157
22. Barretto C, Parreira R, Goncalves R (2008) Platinum nanoparticles embedded in layer-by-layer films from SnO2/polyallylamine for ethanol electrooxidation. J Power Sources 185:6–12
23. Ye F, Li J, Wang T, Liu Y, Wei H, Li J, Wang X (2008) Electrocatalytic properties of platinum catalysts prepared by pulse electrodeposition method using SnO2 as an assisting reagent. J Phys Chem C 112:12894–12898
24. Wu G, Li L, Xu B (2004) Effect of electrochemical polarization of PtRu/C catalysts on methanol electrooxidation. Electrochim Acta 50:1–10
25. Watanabe M, Motoo S (1975) Electrocatalysis by ad-atoms: Part III. Enhancement of the oxidation of carbon monoxide on platinum by ruthenium ad-atoms. J Electroanal Chem 60:275–283
26. Liang Y, Zhang H, Zhong H, Zhu X, Tian Z, Xu D, Yi B (2006) Preparation and characterization of carbon-supported PtRuIr catalyst with excellent CO-tolerant performance for proton-exchange membrane fuel cells. J Catal 238:468–476
27. Lasia C (2012) Dynamic impedance study of ethanol and acetaldehyde oxidation at platinum in acid solutions. Electrochim Acta 78:286–293
28. Melnick RE, Palmore GTR (2001) Time-dependent impedance of the electro-oxidation of methanol on polished polycrystalline platinum. J Phys Chem B 105:9449–9457